Crystalline Effects on the Properties of the Dative Bond: A Computational Study of $HCN-BF_3$

Gerhard Venter and Jan Dillen*

Department of Chemistry, University of Stellenbosch, Private Bag X1, Matieland 7602, South Africa

Received: April 17, 2004; In Final Form: August 3, 2004

The changes in molecular structure associated with the crystallization of the donor−acceptor complex $HCN-BF_3$ are studied using density functional theory. Short-range dipole−dipole interactions have been attributed to be one of the main causes of the 0.84 Å shortening of the B−N bond in the crystal phase compared to the gas phase. Natural bond orbital analysis is used to obtain information regarding the electron distribution and possible delocalization effects. The lone pair on the fluorine atoms shows significant delocalization toward the boron−nitrogen antibonding orbital, leading to substantial structural changes occurring that can be manipulated by increasing or decreasing the degree of overlap. Because the overlap is dependent on the position of the fluorine atom, the steric and electronic influences created by the surroundings of a molecular unit in the crystal are of considerable importance when the experimentally observed changes are explained.

I. Introduction

In general, structural differences between covalently bound molecules in the gas phase and crystal phase are in the order of hundredths of ångstroms.[1] The changes that do occur are usually attributed to crystal packing effects. Donor−acceptor bonds, however, frequently show larger interatomic separations in the gas phase compared to the crystal phase.[2] At the far end of these phase-dependent linkages are the datively bound complexes, such as the Lewis acid−base complex between BF_3 and HCN, which show evidence of bonds forming only partially in the gas phase.[3,4] These bonds are believed to be driven to completion in the crystalline state. In these cases the distinction between partially and fully formed bonds is made on the basis of the sum of the covalent radii for nitrogen and boron, 1.58 Å,[5] and the van der Waals radius, as determined from the bonding distance of the van der Waals complex between molecular nitrogen and boron trifluoride, 2.88 Å.[6] Due to the resulting change in the nature of the bonds, dramatic decreases in bond lengths and associated bond angles are observed. In the case of the complex studied in this paper, the B−N bond retraction is 0.84 Å and the NBF angle widens by 14°.[7,8] Similar changes are known for the related boron−nitrogen adduct CH_3-$CN-BF_3$, where the values are 0.38 Å and 10°,[9,10] respectively.

In the crystal structure of $HCN-BF_3$ the molecules are arranged in pairs such that each two $HCN-BF_3$ molecules are antiparallel to another, at about 3.8 Å away. It has already been shown by Cabaleiro-Lago and Ríos[11] that the changes in the length of the B−N bond upon crystallization can be reproduced to a large extent by the addition of only one additional molecule to form an antiparallel dimer. Their B3LYP/6-31++G** calculations on a $(HCN-BF_3)_2$ dimer reproduced the experimentally observed changes between the gas phase and the crystalline state to within 0.1 Å and 4°. Jiao and Schleyer used self-consistent reaction field (SCRF) theory[12] based on the Onsager reaction field[13,14] to represent the environment as a dielectric continuum, using H_2O as solvent at 25 °C. They calculated the dipole moment of $HCN-BF_3$ as a function of the dielectric constant, ϵ, and found that a change in polarity of the medium influences both the solvation energy and the B−N bond distance to a great extent. From this correlation they concluded that the gas−solid phase changes for this very polar species are mainly due to the dipolar crystal field. A comparative study of a number of Lewis acid−base complexes was done by Jonas, Frenking, and Reetz.[2] Only the gas-phase molecule was calculated in their work; however, geometry optimizations on the dimer and tetramer form of H_3N-BH_3 and the dimer of H_3N-BF_3 showed significantly shorter bonds compared to the monomers. This shortening of the dative bond was attributed to short-range dipolar effects. However, the alignment of molecules in their calculations does not reflect the actual crystallographic structure. Their calculations were done on systems in which the dimeric or tetrameric units were specifically built to maximize the possibility of dipolar interactions (i.e., antiparallel alignment of all molecules throughout the model).

Nearest neighbor effects on the structure are not limited to the crystal phase, as was recently shown by Fiacco and Leopold.[15] They investigated microsolvation effects in the complex $HCN\cdots HCN-BF_3$ by both rotational spectroscopy and ab initio methods and found an experimental B−N bond distance of 2.299 Å. This represents a contraction of 0.174 Å relative to the isolated monomer, caused by a single HCN unit hydrogen bonded to $HCN-BF_3$, 2.185 Å away.

In this paper we investigate the structural changes brought on by a single nearest neighbor, as well as the additive effect of additional units in the crystal structure. An explanation for the well correlated relationship between the B−N bond distance and the NBF angle is presented.

II. Computational Methods

Calculations were performed with both *Gaussian 98*[16] and *Gaussian 03*.[17] The gas-phase $HCN-BF_3$ monomer was optimized with both ab initio and density functional methods as well as a wide range of basis sets. Levels of theory included MP2,[18] the hybrid DFT functionals B3LYP[19,20] and MPWK1[21]

* Corresponding author. E-mail: jlmd@sun.ac.za.

10.1021/jp048319j CCC: $27.50
Published on Web 09/04/2004

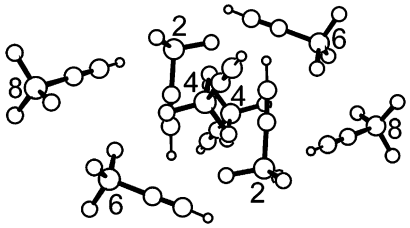

Figure 1. $(HCN-BF_3)_n$ model with $n = 2, 4, 6, 8$. The molecules are numbered such that for a specific value of *n*, the model consists of all the molecules numbered *n* and lower, e.g., for $n = 6$, molecules numbered 2, 4, and 6 are included.

and the pure DFT functional MPWPW91.[22,23] Basis sets ranged from double-ζ 6-31G(d)[24] to triple-ζ 6-311+G(d,p).[25] Crystal phase effects were simulated by adding an environment of frozen $HCN-BF_3$ molecules around a central dimer unit. The coordinates for the surrounding molecules were taken from the crystal structure.[8] To retain the local symmetry within the crystal, which was determined to be C_i, the molecules were added in a pairwise fashion. Taking the point of inversion as the center of the system, all molecules, excluding the central dimer, having at least one atom within a selected radius, were taken as the frozen surroundings. The radius of inclusion was enlarged to encompass more molecules to increase the size of the model system. This procedure was continued until a total size of eight molecules had been reached. Figure 1 illustrates the different crystal models. A number of calculations were also done on the isolated dimer, with the purpose of determining at which intermonomer distance the observed bond shortening occurs. The effect of a varying parallel dipole was also investigated. Stationary points on the potential energy surface were characterized as minima by the absence of imaginary/negative frequencies in the analytically determined vibrations.

Electronic analysis of the system was carried out according to the natural bond orbital (NBO) approach of Weinhold et al.[26,27] Apart from calculating the best NBO natural Lewis structure for an electronic system, this analysis by default includes an estimate of all possible donor−acceptor interactions within the system. This is done by examining all possible interactions between filled Lewis-type NBO's and empty non-Lewis NBO's and estimating their importance by second-order perturbation theory. All NBO calculations were done with the *NBO 5.0* program.[28]

III. Results and Discussion

Within the C_{3v} symmetry group, optimization of the monomer revealed a B−N dative linkage of 2.473 Å, in agreement (albeit possibly a result of a fortuitous cancellation of errors, rather than a reflection of the basis set quality) with the experimental structure, and an NBF angle of 93.0°, comparing reasonably well with the experimentally determined angle of 91.5°.[7] The work of Giesen and Phillips[29] has shed much light on the discrepancy between experimental and theoretical geometries of the related compound, CH_3CN-BF_3. The authors concluded that a very flat potential energy surface (PES) for the B−N stretching coordinate arises from two competing minima, one between 1.8 and 1.9 Å, the other between 2.2 and 2.3 Å. It was shown that basis set superposition error (BSSE) influences the calculations to a huge extent, rendering calculations with smaller basis sets nearly meaningless, and even changing the global minimum for the large cc-aug-PVTZ basis set from the short to the long minimum. It is very likely that similar behavior will be present for the $HCN-BF_3$ moiety. Recently, Gilbert[30] concluded that the B3LYP model performs poorly when used to model dative B−N bonds and suggested the use of the hybrid MPW1K model, which was designed to describe incompletely bound transition states. A comparison between MP2 calculations and B3LYP, MPW1K, and the related pure MPWPW91 applied for a variety of basis sets, for the monomer and dimer, is summarized in Tables 1 and 2.

TABLE 1: Optimized B−N Distances of C_{3v} $HCN-BF_3$ for Various Levels of Theories and Basis Sets[a]

	MP2	B3LYP	MPWK1	MPWPW91
6-31G(d)	2.439	2.473	2.287	2.416
6-31+G(d)	2.430	2.511	1.806	1.854
6-31G(d,p)	2.443	2.474	2.285	2.417
6-31+G(d,p)	2.437	2.512	1.805	1.854
6-311G(d)	2.493	2.494	2.285	2.416
6-311+G(d)	2.435	2.483	1.882	2.296
6-311G(d,p)	2.503	2.495	2.288	2.418
6-311+G(d,p)	2.447	2.484	1.887	2.302

[a] Distances in Å.

TABLE 2: Optimized B−N Distances of the C_i $(HCN-BF_3)_2$ Dimer for Various Levels of Theories and Basis Sets[a]

	B3LYP	MPWK1	MPWPW91
6-31G(d)	1.806[b]	1.735	1.762
6-31+G(d)	1.735	1.697	1.720
6-31G(d,p)	1.800	1.732	1.757
6-31+G(d,p)	1.736	1.698	1.721
6-311G(d)	2.330	1.750	1.802
6-311+G(d)	1.772	1.713	1.741
6-311G(d,p)	2.329	1.751	1.800
6-311+G(d,p)	2.484	1.715	1.743

[a] Distances in Å. [b] A second, higher energy minimum with C_2 symmetry and $r(B-N) = 2.287$ Å was also found doing the dimer intermolecular separation, as discussed later.

Table 1 illustrates the good performance of B3LYP compared to MP2, and although there does not seem to be any convergence relative to the chosen basis, *it does display a degree of consistency*. The other two functionals display similar behavior, as observed by Giesen and Phillips, in that the addition of diffuse functions drives the monomer to a short minimum of ca. 1.8 Å, as compared to the longer minimum at ca. 2.2−2.4 Å. Whereas the calculations by Giesen and Phillips also indicated inconsistency in the MP2 results, we obtained none. These authors, however, did rigorous calculations on the PES of the respective molecules by doing stepwise partial optimizations of the B−N stretching coordinate. The scope of this article is not to provide a similar account of $HCN-BF_3$, and the minima reported in Tables 1 and 2 might not be global in all cases. Having said this, optimizations of the monomer were done with starting coordinates corresponding to a B−N bond distance of 1.6 Å to span the whole region of possible minima, but this is not a guarantee that the minima found are global. The consistency of B3LYP disappears in the case of the dimer. Here two different minima are found once again, whereas the other two functionals display consistency relative to the basis set.

The effect of BSSE on the energy was calculated for all the basis sets used in the B3LYP monomers and found to show relatively little sensitivity to the size of the basis set, but once again to the availability of diffuse functions. The basis sets (in order of increasing size) without diffuse functions have values of 2.06, 2.06, 1.79, and 1.75 kcal/mol, whereas those with diffuse functions have 0.58, 0.60, 0.70, and 0.64 kcal/mol. High values of BSSE thus seem to correlate with long minima, and vice versa for low values of BSSE. It is also of value to note that the BSSE energy for the basis set used in the cluster calculations amounts to between one-half and one-third of the

TABLE 3: Structural Data for $(HCN-BF_3)_2$, $n = 2, 4, 6, 8$[a]

	$(HCN-BF_3)_2$	$(HCN-BF_3)_4$	$(HCN-BF_3)_6$	$(HCN-BF_3)_8$
BN	1.806	1.739	1.670	1.665
NBF···H[b]	99.3	100.3	102.1	103.8
NBF	102.3	103.6	105.6	103.5
NBF	102.5	104.5	105.6	106.1

[a] Distances in Å, angles in deg. [b] The NBF angle of the F hydrogen bonded to the opposite antiparallel molecule.

complex dissociation energy, which was calculated to be 4.8 kcal/mol, and could be even worse for the larger clusters. This probably has little effect on the structural results for the clusters but some caution is nonetheless warranted.

Due to the flat PES, without a good description of gradients at each optimization step, the dimer models do not converge easily. Unfortunately, procedures to remedy this behavior increase the computational time considerably, even more so with large basis size. Because we are only interested in the qualitative effect of additional molecules on the dimer, we decided on B3LYP/6-31G(d) being a sufficient approach with the assumption that any computational discrepancies are present in all the $(HCN-BF_3)_n$ crystal models.

Intermolecular Effects. Table 3 lists some important bond lengths and bond angles indicating the changes in structure that were induced by increasing the number of surrounding molecules. Figure 1 illustrates how the molecules were arranged. Upon going from the monomer to the dimer, thus the addition of only one molecule, the B−N bond length decreases from 2.473 to 1.806 Å, a difference of 0.667 Å. As expected, the NBF angles widen by between 6 and 9°. The formation of a hydrogen bond between the hydrogen atom and the opposing fluorine, as well as the application of overall C_i symmetry leads to the local 3-fold axis that exists in the isolated molecule to be destroyed in the dimer, resulting in the NBF angles differing slightly. The NBF angle containing the hydrogen-bonded F-atom is smaller than the remaining two in the molecule. However, as the amount of surrounding molecules increases, and hence more hydrogen bonds are formed between the dimer unit and surrounding H-atoms, the remaining two angles also display differences. Defining the NBF angle containing the F-atom hydrogen bonded to the opposite molecule in the dimer as the inward pointing angle, and the two remaining angles as the outward pointing angles, a clear illustration of the surrounding molecule effect is the difference between the outward pointed NBF angles in the $(HCN-BF_3)_6$ and $(HCN-BF_3)_8$ systems. As seen in Figure 1, the latter system differs from the former system by the two molecules labeled 8. These two added molecules result in an additional hydrogen bond to an F-atom, distorting the two outward pointing NBF angles to 103.5° and 106.1°, compared with the equal NBF angles of 105.6° in the $(HCN-BF_3)_6$ system.

From $(HCN-BF_3)_2$ to $(HCN-BF_3)_8$ a further 0.141 Å, or 17%, decrease in B−N bond length occurs. Although changes of this order are considered to be of fundamental importance, it is still largely overshadowed by the changes observed in the dimer. Hankinson, Almlöf, and Leopold[31] have determined dipole−dipole interactions between a $HCN-BF_3$ molecule and one nearest antiparallel neighbor account for one-third of the lattice energy. They also showed the molecular dipole moment to be a sensitive indicator of the degree of completion of the dative bond. Their findings are reflected by our B3LYP/6-31G* calculated values: the dipole moment of the isolated monomer calculated with a fixed B−N of 2.4 Å is 4.3 D, compared to a dipole of 7.4 D at a fixed B−N distance of 1.6 Å. The fact that the dipole moment can be manipulated by changing the B−N bond length, allowed us to do a simple test of the sensitivity of the molecule to the dipole moment of an antiparallel molecule. A dimer was optimized without any symmetry constraints while the boron−nitrogen bond length of one molecule was kept fixed. The dipole moment of this molecule, calculated with the geometry it has in the partially optimized dimer, was also established. Figure 2 shows the bond length of the other, fully optimized molecule in the dimer as a function of the dipole moment of the molecule with the frozen B−N bond. Taking the two molecules in the dimer to be labeled **A** and **B**, a fixed *r*(BN) of 2.473 Å in **A** results in a molecular dipole of 4.1 D in **A**. Molecule **B** optimizes to a bond length of 1.863 Å with a resulting molecular dipole of 6.4 D. At the upper end of the graph, a fixed *r*(BN) of 1.673 Å in **A** results in the opposing molecule **B** optimizing to *r*(BN) = 1.794 Å. Other effects that might influence the structure, such as hydrogen bonding, are of course also apparent in this approach. However, bond length decreases of this order have previously[2,32] been attributed to dipole−dipole interactions.

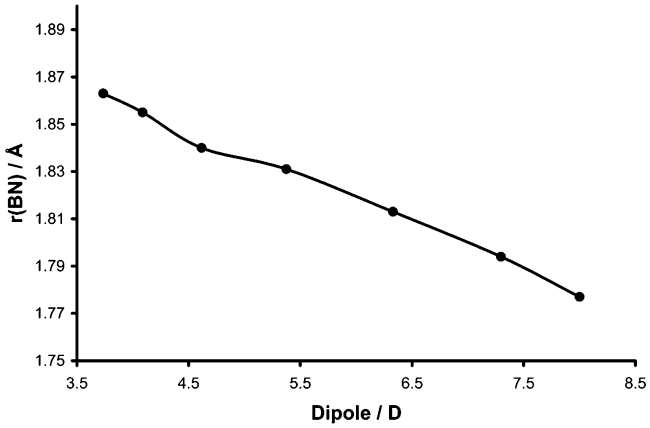

Figure 2. Bond length of one BN bond in $(HCN-BF_3)_2$ as a function of the molecular dipole moment of the opposing, antiparallel molecule. To present a varying dipole moment, the dimer was optimized with one *r*(BN) fixed in steps of 0.2 Å, from 2.673 to 1.473 Å.

Before further conclusions are made regarding the importance of dipolar interaction in the molecular clusters modeled by us and other groups, one needs to carefully reassess the effect of dipole orientation. Simplifying to point dipoles, the classical potential energy of interaction between dipoles is given by[33]

$$V(r) = \frac{\boldsymbol{\mu_1}\cdot\boldsymbol{\mu_2}}{4\pi\epsilon_0 r^3} - 3\frac{(\boldsymbol{\mu_1}\cdot\mathbf{r})(\boldsymbol{\mu_2}\cdot\mathbf{r})}{4\pi\epsilon_0 r^5}$$

In this equation, $\boldsymbol{\mu_1}$ and $\boldsymbol{\mu_2}$ are two vectors representing the interacting dipoles, whereas **r** is a vector connecting the center of the two dipoles. According to this equation, the potential energy is a maximum when the dipole moments are parallel (i.e., an angle of 0° between their respective dipole moment vectors) and directly opposite each other (i.e., an angle of 90° between the vector **r** connecting the point dipoles and the dipole moment vector). Figure 3 shows the unit cells for the molecules mentioned so far. In crystalline H_3N-BH_3 all the molecules are arranged parallel, i.e., orientated in the same direction. This picture differs largely from the $HCN-BF_3$ crystal. Here the molecules *in a dimeric unit* are aligned antiparallel; i.e., their dipole moment vectors are aligned 180° with respect to each other. However, the different dimer units are aligned near orthogonal with respect to each other (see Figure 1), resulting in small values for the potential energy of interaction. A similar arrangement is observed in the H_3N-BF_3 crystal. To attribute

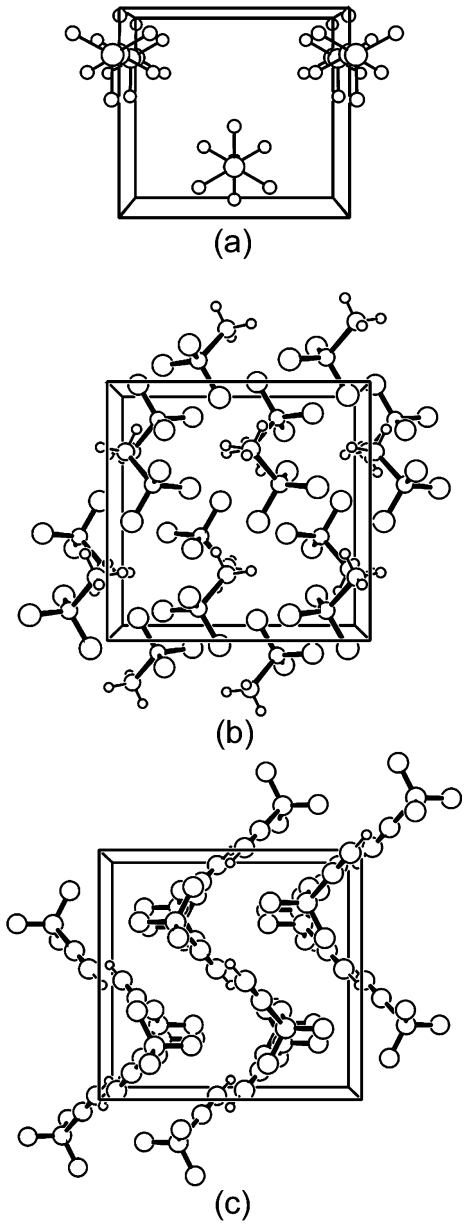

Figure 3. Crystallographic unit cells for (a) H_3N-BH_3, (b) H_3N-BF_3, and (c) $HCN-BF_3$. Note the difference in orientation of the molecules in the unit cells. In H_3N-BH_3 all molecules are aligned parallel. The other two cells consist of dimeric units which are aligned antiparallel, but no parallel interdimer alignment.

a decrease of 0.141 Å brought on by 6 surrounding molecules that are aligned in such a way to nearly minimize the possible dipolar interaction to solely dipole−dipole effects, thus seems doubtful.

Hydrogen bonding may be one of the alternative effects responsible for the changes in the crystal. Merino, Bakhmutov, and Vela[34] have recently concluded that proton−hydride interactions in $(H_3B-NH_3)_2$ are not the main factors influencing the 0.077 Å change in dative bond length experimentally observed for this system. They concurred with previous work in that dipole−dipole interactions are primarily responsible.[2,32] This does seem a logical conclusion, as in this case the dipole moments are arranged parallel/antiparallel (i.e., angles of 0° or 180°, respectively) in the crystal. For $(HCN-BF_3)_2$, we determined whether H···F contacts were responsible for the changes by the very simple procedure of removing all H's from the system and replacing them with F-atoms. This hypothetical

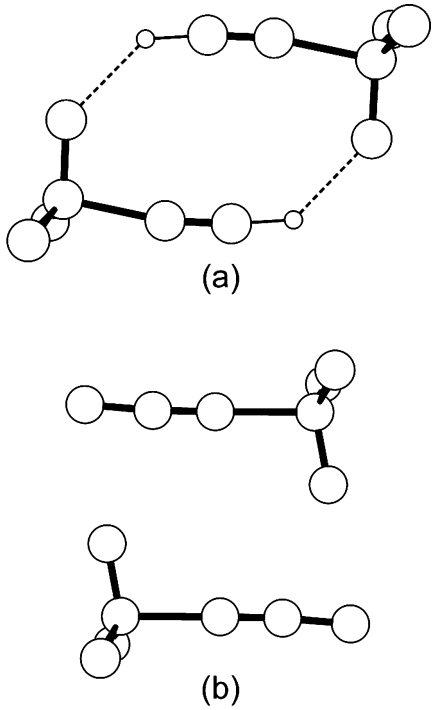

Figure 4. (a) $(HCN-BF_3)_2$ and (b) $(FCN-BF_3)_2$ at B3LYP/6-31G*. Note the larger intermolecular separation in $(FCN-BF_3)_2$, as well as the deviation from linearity observed in the HCN−B molecular axis compared to the FCN−B molecular axis.

dimer, $(FCN-BF_3)_2$, was optimized at B3LYP/6-31G* and its geometry compared with the isolated $FCN-BF_3$ molecule. In the monomer, which has C_{3v} symmetry, the B−N bond is calculated to be 2.519 Å, compared to 1.834 Å in the dimer, which has C_{2h} symmetry. The remarkable change in structure is thus still evident in a completely fluorinated compound, without the possibility of any hydrogen bonding. Replacing the H's with F's, however, does not eliminate the possibility of strong intermolecular interaction. The different deviations from linearity observed in the molecular axis for the two molecules indicate geometry deforming interactions in both species, but of a different nature, i.e., attractive H···F hydrogen bonding in $(HCN-BF_3)_2$ vs a repulsive F···F electrostatic interaction in $(FCN-BF_3)_2$. Figure 4 shows the B−NCH axis bending toward the antiparallel molecule as opposed to the B−NCF axis, which in fact bends away from the antiparallel molecule. The molecular dipole moment for the monomer was calculated to be 3.4 D, and for the isolated dimer, 6.0 D.

A further clue into the bond-shortening mechanism can be taken from calculating the change in structure taking place in a $HCN-BF_3$ molecule as a second, antiparallel molecule approaches. This was done by doing a set of partial optimizations in which the perpendicular distance between the molecules was kept fixed, from 3.5 to 5.0 Å, in steps of 0.1 Å. Figure 5 illustrates the change in dative bond length as a function of the perpendicular intermolecular separation. In doing the separation a second minimum was identified with a B−N bond length of 2.287 Å, compared to the minimum at 1.807 Å.[35] The calculations were done without symmetry constraints, resulting in both minima having a symmetry (C_2) different from that of the results reported in Table 2. The most notable result from the graph is that the bond shortening is not linearly dependent on the separation. A sudden jump occurs between $r(d) = 4.5$ Å and $r(d) = 4.6$ Å. At a separation of 4.6 Å the dative bond length is 2.398 Å, which shortens to 1.914 Å at a separation of 4.5 Å. The molecule is increasingly stabilized by the approaching unit

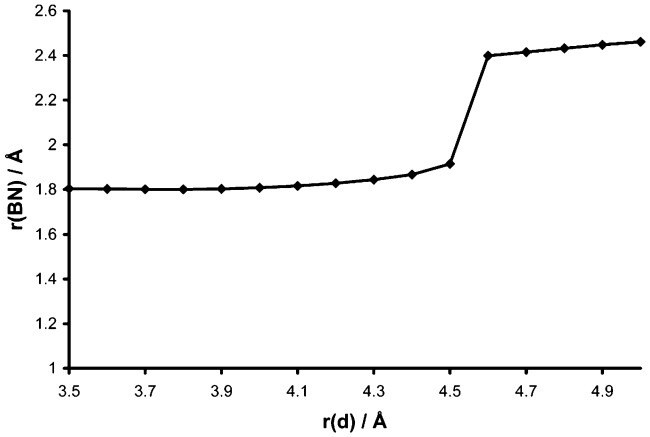

Figure 5. r(BN) as a function of $r(d)$ in $(HCN-BF_3)_2$, where $r(d)$ is the perpendicular distance between the two molecules in the dimer.

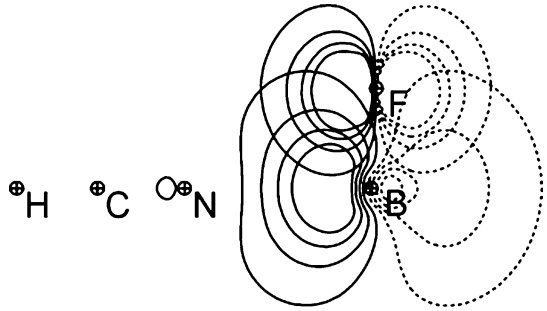

Figure 6. Contour illustration of the n(F) → σ*(BN) delocalization in $HCN-BF_3$. The overlap shown is that of the nonorthogonal pre-NBO's, which differ from the orthogonal NBO's only in the absence of the "orthogonality tails".[26]

up to the point where the molecules promptly progress to a more genuine dative interaction. These observations are discussed in more detail and rationalized when the molecular orbitals are discussed, in a later section.

Intramolecular Effects. Second-order perturbative estimates of the interaction between filled and empty orbitals in the NBO basis of $HCN-BF_3$ reveal a large value of 39.7 kcal/mol for the stabilization energy resulting from the delocalization of one lone pair on the F-atom to the B−N antibonding orbital. Overlap of the three equivalent fluorine lone pairs leads to a significant occupation of the destabilizing antibonding B−N orbital of 0.33 e. This is without doubt a major contributing factor to the weaker B−N bonding interaction and a resulting longer bond in the gas-phase monomer. Figure 6 illustrates the n(F) → σ*(BN) overlap. This looks somewhat similar to, but should not be confused with, the well-known π-overlap in BX species that leads to *stronger* B−X bonds and has been used to explain the relative strengths of the boron halides as Lewis acids.[36,37] The optimal natural Lewis structure for isolated BF_3 as determined by die NBO partitioning scheme does indeed show a π-bond due to the above-mentioned overlap, but this stabilizing interaction is absent (as expected) in the bonded $HCN-BF_3$ species.

The importance of this delocalization to the geometry of the complex can be estimated by removing the relevant elements from the NBO Fock matrix and calculating a new density matrix to be used in the SCF evaluator. Within *Gaussian 98* this can be done by first identifying the overlap elements of interest from the second-order perturbation theory analysis section of the output and then doing a calculation with *pop=nbodel* in the route section, together with the elements in a separate section of the input file.[38] A geometry optimization done in this way results in a B−N bond length of 1.501 Å, illustrating the effect of the fluorine lone pairs on the structure of the molecule. Also, if the fluorine lone pairs are instrumental in the mechanism, one should not see any significant bond shortening in a similar system, but with the lone pairs absent. This was investigated by replacing the F atoms with H atoms and optimizing the resulting $HCN-BH_3$ and $(HCN-BH_3)_2$ complexes at B3LYP/6-31G*. Indeed, as expected, the monomer bond length of 1.544 Å shortened by "only" 0.033 Å to 1.511 Å in the dimer. Although a change of 0.033 Å is by far not irrelevant, it is small compared to the order observed in $HCN-BF_3$. NBO analysis also shows a nearly unoccupied antibonding orbital for both the monomer and dimer (0.007 e).

The B−N bond length is thus shortened or lengthened, respectively, by the increasing or decreasing availability of a fluorine lone pair for overlap with the antibonding natural orbital of the bond. Instead of removing the lone pairs in total, the lone pair availability can also be adjusted by either increasing the B−F bond length, or by widening the NBF angle, to move the fluorine atom further away from the B−N bond. Hankinson, Almlöf, and Leopold have already illustrated this dependence of the B−N bond length on the NBF angle and B−F bond distance by doing R-fixed and α-fixed optimizations on $HCN-BF_3$ (R = B−N bond distance, α = NBF angle).[10,31] Although this relationship can be explained by simple VSEPR theory, we have now provided a further explanation in terms of the purely theoretical concept of orbital overlap.

An explanation for the gas/crystal phase differences, which explains the additional structural changes brought on by surrounding molecules, follows. Any external factors resulting in a deformation of the geometry of the BF_3 fragment from its equilibrium planar D_{3h} geometry to its bonded pyramidal C_{3v} geometry will create an environment that is more susceptible to donation from a Lewis base. In the crystal, hydrogen bonds are formed between neighboring molecules. From Figure 1 it can be seen that the NBF angles increase as more H···F contacts are established in the crystal, lowering the total delocalization of fluorine lone pairs to the antibonding B−N orbital. As more molecules are added, the deformation increases. This effect reaches a maximum when no more H···F contacts are possible. NBO energetic analysis confirms this by indicating progressively lower values for n(F) → σ*(BN) as the $(HCN-BF_3)_n$ model increases in size. The formation of only a partial bond in the gas phase may then be explained as a result of the inability of the approaching donor, in this case HCN, to deform the geometry of the BF_3 to such a degree that full bonding is possible. The observations above may be formulated as follows: *in general any interaction, whether steric or electronic, that results in the atom that contains the lone pair(s) moving further away from the dative bond, so that the possibility of lone pair donation into the antibonding orbital is minimized, should result in a stronger bond for the system.*

Care must, however, be taken in generalizing this statement. Dillen and Verhoeven recently used a method similar to the one we employed to calculate H_3N-BH_3 in an environment closely resembling the true crystal.[32] They were able to calculate changes in structure of at most 0.08 Å as a consequence of neighboring molecules. Jonas, Frenking, and Reetz calculated a 0.058 Å decrease in bond length going from their monomer to tetramer structure.[2] The experimentally observed change is from 1.657 Å in the gas phase to 1.58 Å in the crystal phase.[39,40] This molecule is thus an example of substantial changes in structure in the absence of lone pair delocalization, although the advantageous dipole arrangement probably plays a large role in this system. H_3N-BF_3 shows an *increase* in experimental

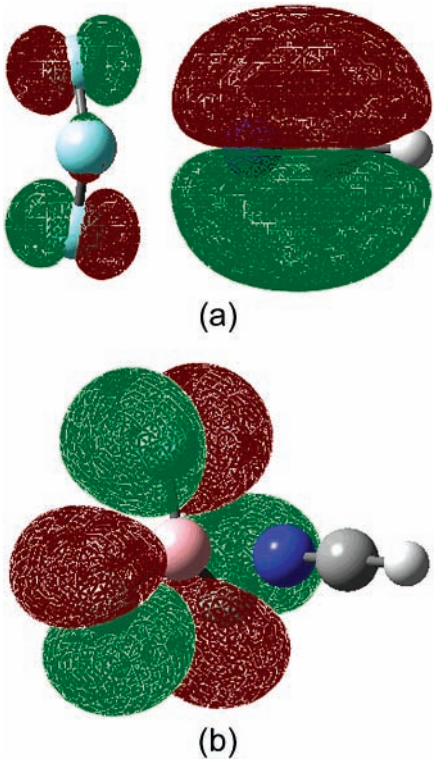

Figure 7. Highest occupied molecular orbitals (HOMO's) for HCN−BF_3, calculated at (a) MPWK1/6-311G(d,p) and (b) MPWK1/6-311+G-(d,p).

bond length between the gas and crystal phase, from 1.59 to 1.60 Å, illustrating that lone pair influences are not always significant.[41,42] Jonas, Frenking, and Reetz determined a 0.05 Å bond length decrease in their dimeric H_3N-BF_3 model.[2]

One remaining question still needs attention, how the addition of a diffuse function leads to different minima on the PES, seemingly independent of the size of the basis set. This is evident throughout most of the basis sets and levels of theory shown in Table 1, but because the MPWK1 calculations provide the most extreme example of this, those results were used as a representative set. The valence molecular orbitals (MO's) of the eight different minima were calculated. The shapes of the MO's do remain nearly similar for both minima, the energy ordering of the higher lying orbitals, however, differs. The shorter bonded minima (with diffuse functions) have HOMO's consisting of largely localized fluorine lone pair orbitals and the longer minima (without diffuse functions) have their HOMO density delocalized between the lone pairs and the π-system of the HCN. The HOMO's for two representative basis sets are shown in Figure 7. From these one clearly sees the different descriptions provided by the basis sets. Because diffuse functions play the dominant role in describing accurate electron distributions for negatively charged species or atoms with high electronegativities, their effect comes as no surprise once the importance of the lone pairs in the bond length is elucidated.

The sudden jump occurring in the dimer intermolecular separation (Figure 5) can now be explained in terms of the observations given above. As reported earlier, two minima, with B−N bond lengths of 1.807 and 2.287 Å, respectively, were obtained. Comparison between the MO's of these minima show a rearrangement similar to that of the monomer; i.e., the HOMO of the dimer with short B−N bonds consists of localized lone pairs whereas the other one is more delocalized. The quantized nature of MO's and their energies thus explain the sudden jump as the occupied MO's of the HCN−BF_3 molecules are rearranged.

IV. Conclusions

We have examined the changes in structure brought on by neighboring molecules in the HCN−BF_3 crystal. Different models were constructed, in which the number of molecules were increased in a pairwise fashion around a central dimer unit. Calculations were done at the B3LYP/6-31G* level of theory. The conclusion reached by Cabaleiro-Lago and Ríos,[11] that the structural changes occurring upon crystallization are due to a cooperative effect involving the closest molecules to each individual ones, was reaffirmed. We have also shown that additional molecules beyond the dimer account for a further 17% decrease in bond length (compared to the experimentally determined total bond shortening) and that their influence is certainly not negligible. The changes due to one nearest neighbor can certainly be a result of dipole−dipole interactions, as the molecule was shown to be extremely sensitive to nearby dipoles. However, the near orthogonal orientation of the dipoles beyond the central dimer with respect to the central unit, suggests that an additional mechanism might also be present which we believe is given by NBO analysis. Significant delocalization of the fluorine lone pairs into the antibonding orbital of the B−N bond results in a very high occupation of this orbital in the isolated molecule. The degree of delocalization is lessened as the NBF angle is increased, giving a qualitative explanation for the previously determined relationship between the B−N bond and the NBF angle.[10,31] The difference between the gas phase structure and the crystal structure is thus explained to be a consequence of the structurally decisive intramolecular delocalization of the fluorine lone pairs, which is lessened in the crystal structure, accompanied by short-range dipole−dipole interactions. Hydrogen-bonding and steric effects in the crystal result in a larger distortion of the NBF angle and thus a smaller n(F) → σ^*(BN) overlap. This drives the bond formation to completion and shortens the bond to values normally found in covalent bonds.

Acknowledgment. This research was supported by the National Research Foundation (NRF), grant 2053646.

Supporting Information Available: Text file with coordinates of the partial optimizations of the crystal cell, the C_2 dimer minima, and the **Z**-matrix for the stepwise separation optimization. This material is available free of charge via the Internet at http://pubs.acs.org.

References and Notes

(1) Hargittai, M.; Hargittai, I. *Phys. Chem. Miner.* **1987**, *14*, 413.
(2) Jonas, V.; Frenking, G.; Reetz, M. T. *J. Am. Chem. Soc.* **1994**, *116*, 8741.
(3) Leopold, K. R. In *Advances in Molecular Structure Research*; Hargittai, M., Hargittai, I., Eds.; JAI Press: Greenwich, CT, 1996; Vol. 2, p 103.
(4) Leopold, K. R.; Canagaratna, M.; Phillips, J. A. *Acc. Chem. Res.* **1997**, *30*, 57.
(5) Muetterties, E. L. *The Chemistry of Boron and its Compounds*; Wiley: New York, 1967.
(6) Janda, K. C.; Bernstein, L. S.; Steed, J. M.; Novick, S. E.; Klemperer, W. *J. Am. Chem. Soc.* **1978**, *100*, 8074.
(7) Reeve, S. W.; Burns, W. A.; Lovas, F. J.; Suenram, R. D.; Leopold, K. R. *J. Phys. Chem.* **1993**, *97*, 10630.
(8) Burns, W. A.; Leopold, K. R. *J. Am. Chem. Soc.* **1993**, *115*, 11622.
(9) Swanson, B.; Shriver, D. F.; Ibers, J. A. *Inorg. Chem.* **1969**, *8*, 2182.
(10) Dvorak, M. A.; Ford, R. S.; Suenram, R. D.; Lovas, F. J.; Leopold, K. R. *J. Am. Chem. Soc.* **1992**, *114*, 108.

(11) Cabaleiro-Lago, E. M.; Roís, M. A. *Chem. Phys. Lett.* **1998**, *294*, 272.
(12) Jiao, H.; Schleyer, P. v. R. *J. Am. Chem. Soc.* **1994**, *116*, 7429.
(13) Wong, M. W.; Frisch, M. J.; Wiberg, K. B. *J. Am. Chem. Soc.* **1991**, *113*, 4776.
(14) Wong, M. W.; Wiberg, K. B.; Frisch, M. J. *J. Am. Chem. Soc.* **1992**, *114*, 4.
(15) Fiacco, D. L.; Leopold, K. R. *J. Phys. Chem. A* **2003**, *107*, 2808.
(16) Frisch, M. J.; Trucks, G. W.; Schlegel, H. B.; Scuseria, G. E.; Robb, M. A.; Cheeseman, J. R.; Zakrzewski, V. G.; Montgomery, J. A., Jr.; Stratmann, R. E.; Burant, J. C.; Dapprich, S.; Millam, J. M.; Daniels, A. D.; Kudin, K. N.; Strain, M. C.; Farkas, O.; Tomasi, J.; Barone, V.; Cossi, M.; Cammi, R.; Mennucci, B.; Pomelli, C.; Adamo, C.; Clifford, S.; Ochterski, J.; Petersson, G. A.; Ayala, P. Y.; Cui, Q.; Morokuma, K.; Salvador, P.; Dannenberg, J. J.; Malick, D. K.; Rabuck, A. D.; Raghavachari, K.; Foresman, J. B.; Cioslowski, J.; Ortiz, J. V.; Baboul, A. G.; Stefanov, B. B.; Liu, G.; Liashenko, A.; Piskorz, P.; Komaromi, I.; Gomperts, R.; Martin, R. L.; Fox, D. J.; Keith, T.; Al-Laham, M. A.; Peng, C. Y.; Nanayakkara, A.; Challacombe, M.; Gill, P. M. W.; Johnson, B.; Chen, W.; Wong, M. W.; Andres, J. L.; Gonzalez, C.; Head-Gordon, M.; Replogle, E. S.; Pople, J. A. *Gaussian 98*, A.11.3; Gaussian, Inc.: Pittsburgh, PA, 2002.
(17) Frisch, M. J.; Trucks, G. W.; Schlegel, H. B.; Scuseria, G. E.; Robb, M. A.; Cheeseman, J. R.; Montgomery, J. A., Jr.; Vreven, T.; Kudin, K. N.; Burant, J. C.; Millam, J. M.; Iyengar, S. S.; Tomasi, J.; Barone, V.; Mennucci, B.; Cossi, M.; Scalmani, G.; Rega, N.; Petersson, G. A.; Nakatsuji, H.; Hada, M.; Ehara, M.; Toyota, K.; Fukuda, R.; Hasegawa, J.; Ishida, M.; Nakajima, T.; Honda, Y.; Kitao, O.; Nakai, H.; Klene, M.; Li, X.; Knox, J. E.; Hratchian, H. P.; Cross, J. B.; Adamo, C.; Jaramillo, J.; Gomperts, R.; Stratmann, R. E.; Yazyev, O.; Austin, A. J.; Cammi, R.; Pomelli, C.; Ochterski, J. W.; Ayala, P. Y.; Morokuma, K.; Voth, G. A.; Salvador, P.; Dannenberg, J. J.; Zakrzewski, V. G.; Dapprich, S.; Daniels, A. D.; Strain, M. C.; Farkas, O.; Malick, D. K.; Rabuck, A. D.; Raghavachari, K.; Foresman, J. B.; Ortiz, J. V.; Cui, Q.; Baboul, A. G.; Clifford, S.; Cioslowski, J.; Stefanov, B. B.; Liu, G.; Liashenko, A.; Piskorz, P.; Komaromi, I.; Martin, R. L.; Fox, D. J.; Keith, T.; Al-Laham, M. A.; Peng, C. Y.; Nanayakkara, A.; Challacombe, M.; Gill, P. M. W.; Johnson, B.; Chen, W.; Wong, M. W.; Gonzalez, C.; Pople, J. A. *Gaussian 03*, B.05; Gaussian, Inc.: Pittsburgh, PA, 2003.
(18) Møller, C.; Plesset, M. S. *Phys. Rev.* **1934**, *46*, 618.
(19) Becke, A. D. *J. Chem. Phys.* **1993**, *98*, 5648.
(20) Lee, C.; Yang, W.; Parr, R. G. *Phys. Rev. B.* **1988**, *37*, 785.
(21) Lynch, B. J.; Fast, P. L.; Harris, M.; Truhlar, D. G. *J. Phys. Chem. A* **2000**, *104*, 4811.
(22) Adamo, C.; Barone, V. *J. Chem. Phys.* **1998**, *108*, 664.
(23) Perdew, J. P.; Chevary, J. A.; Vosko, S. H.; Jackson, K. A.; Pederson, M. R.; Singh, D. J.; Fiolhais, C. *Phys. Rev. B.* **1992**, *46*, 6671.
(24) Hehre, W. J.; Ditchfield, R.; Pople, J. A. *J. Chem. Phys.* **1972**, *56*, 2257.
(25) Krishnan, R.; Binkley, J. S.; Seeger, R.; Pople, J. A. *J. Chem. Phys.* **1980**, *72*, 650.
(26) Weinhold, F. In *Encyclopdia of Computational Chemistry*; Schleyer, P. v. R., Ed.; Wiley: New York, 1998; Vol. 3, p 1792.
(27) Reed, A. E.; Curtiss, L. A.; Weinhold, F. *Chem. Rev.* **1988**, *88*, 899.
(28) Glendening, E. D.; Badenhoop, J. K.; Reed, A. E.; Carpenter, J. E.; Bohmann, J. A.; Morales, C. M.; Weinhold, F. *NBO 5.0*; Theoretical Chemistry Institute, University of Wisconsin: Madison, WI, 2001.
(29) Giesen, D. J.; Phillips, J. A. *J. Phys. Chem. A* **2003**, *107*, 4009.
(30) Gilbert, T. M. *J. Phys. Chem. A* **2004**, *108*, 2550.
(31) Hankinson, D. J.; Almlöf, J.; Leopold, K. R. *J. Phys. Chem.* **1996**, *100*, 6904.
(32) Dillen, J.; Verhoeven, P. *J. Phys. Chem. A* **2003**, *107*, 2570.
(33) Atkins, P.; de Paula, J. *Atkins' Physical Chemistry*, 7th ed.; Oxford University Press: New York, 2002.
(34) Merino, G.; Bakhmutov, V. I.; Vela, A. *J. Phys. Chem. A* **2002**, *106*, 8491.
(35) The change in symmetry from C_i to C_2 results in the B−N bond length of this minimum being slightly longer than the one reported in Table 2.
(36) Frenking, G.; Fau, S.; Marchand, C. M.; Grützmacher, H. *J. Am. Chem. Soc.* **1997**, *119*, 6648.
(37) Cotton, F. A.; Wilkinson, G. *Advanced Inorganic Chemistry*, 5th ed.; Wiley: New York, 1988.
(38) As explained in the *NBO 5.0* manual, ref 28.
(39) Thorne, L. R.; Suenram, R. D.; Lovas, F. J. *J. Chem. Phys.* **1983**, *78*, 167.
(40) Klooster, W. T.; Koetzle, T. F.; Siegbahn, P. E. M.; Richardson, T. B.; Crabtree, R. H. *J. Am. Chem. Soc.* **1999**, *121*, 6337.
(41) Legon, A. C.; Warner, H. E. *J. Chem. Soc., Chem. Commun.* **1991**, 1397.
(42) Goebbels, D.; Meyer, G. *Z. Anorg. Allg. Chem.* **2002**, *628*, 1799.